

Supporting Information

FEMC-deuterogenic artificial solid electrolyte interphase boosts high-performance sodium-ion batteries

Sicheng Miao ^{a,‡}, Ye Jia ^{a,‡}, Ruoxuan Chen ^a, Yueqi Pan ^a, Jianan Peng ^a, Xuemei Zhang ^{b,*}, and Wenlong Cai ^{a,*}

^a Department of Advanced Energy Materials, College of Materials Science and Engineering, Sichuan University, Chengdu, 610064, China

^b Institute of Smart City and Intelligent Transportation, Southwest Jiaotong University, Chengdu, 610032, China

Department of Advanced Energy Materials, College of Materials Science and Engineering, Sichuan University, Chengdu, 610064, P. R. China

* Corresponding authors: caiwl@scu.edu.cn; xuemei_zhang@swjtu.edu.cn

‡ These authors contributed equally to this work.

Experimental Section

Materials

Battery-grade sodium-ion electrolyte, dimethyl ether (DME), and methyl 2,2,2-trifluoromethyl ester (FEMC) were purchased from Duoduo chemical reagent Co., Ltd. N-methyl pyrrolidone (NMP), Super-P, Al foil, Na plate (Φ 15.6 mm), and polyvinylidene difluoride (PVDF) were purchased from Dongguan Kelude Experimental Equipment Technology Co., Ltd. Whatman GF-C glass fiber was bought in Cytiva Bio-technology(Hangzhou) Co., Ltd.

Preparation of the NaF-rich composite artificial interphase

Initially, the reaction solution (the volume ratio of FEMC to DME is 1:100) was carefully prepared and subsequently applied to the surface of the sodium sheet. After allowing a brief period of 30 seconds, the sheet was gently rinsed with DEC to remove any excess solution. After that, a NaF-rich composite artificial interphase was constructed on the surface of the sodium film (noted as NaF@Na) by reacting spontaneously with the organic solution.

Preparation of electrolytes

The solution consisting of ethylene carbonate (EC) and diethyl carbonate (DEC) with a volume ratio of 1:1 was prepared as a solvent, and the carbonate electrolyte (noted as blank electrolyte) contained 1.0 M NaClO₄ salt into the above solvent with 5% fluoroethylene carbonate (FEC) additive. As for FEMC-added electrolyte, namely a

liquid system composed of blank electrolyte and FEMC additive with a volume ratio of 1%.

Preparation of cathode

Firstly, the slurry of $\text{Na}_3\text{V}_2(\text{PO}_4)_3$ (NVP), Super-P, and PVDF in NMP with a mass ratio of 8:1:1 was coated on Al foil uniformly. After being dried in a vacuum oven at 60 °C overnight, NVP electrodes were collected by cutting the above-dried Al foil into discs with a diameter of 12 mm. The areal mass loading of the circular sheet was about 1.7 mg cm^{-2} .

Electrochemical characterization

The electrochemical performance of different anodes was tested in CR-2032 coin cells. Both sodium ion symmetrical batteries and full cells were assembled with the prepared electrolytes. The amount of electrolyte was 175 μL per coin cell. More precisely, NVP electrodes (Φ 12 mm) and Na plates (Φ 15.6 mm, thickness 400 μm) were used as the working electrodes, and the Na plates (Φ 15.6 mm, thickness 400 μm) were worked as the counter electrodes, the Whatman GF-C glass fiber (Φ 18 mm) was used as a separator. The amount of electrolyte is about 175 μl per coin cell. The Voltage-time profiles during Na plating/stripping were tested at the current density of 0.5 mA cm^{-2} . The Electrochemical impedance spectroscopy (EIS) and Tafel curves were obtained on an electrochemical workstation (CHI 660E). The electrochemical characterizations of the Na || NVP full cells were tested with a voltage range of 2.0–3.8

V (*vs.* Na⁺/Na). All galvanostatic discharge/charge tests were performed using a Neware battery test station (BTS–10V6A) with a voltage range of 2.0–3.8 V (*vs.* Na⁺/Na).

Characterization

X-ray diffraction (XRD) was conducted to investigate the crystal structure of NVP powder and electrodes using Dandong Haoyuan DX-2700BH X-ray diffractometer. The microscopic morphologies of NVP powder were characterized by employing the field emission scanning electron microscope (FESEM, Hitachi, S4800, Japan). The properties and composition of SEI were investigated by X-ray photoelectron spectra (XPS) using the Thermo Scientific K-Alpha instrument. Dynamic deposition morphology of sodium metal was observed by in-situ optical microscopy from YUESCOPE. Atomic force microscopy (AFM, BRUKER, Dimension Icon) was used to obtain the morphologies of the surfaces of NaF@Na and Na electrodes in a glove box.

Density functional theory (DFT) calculations

All calculations were performed within the framework of DFT and the electrocatalytic and electrocatalytic properties of the materials were investigated using the CASTEP module implemented in Material Studio. The theoretical framework was grounded on the Generalized Gradient Approximation (GGA), specifically employing the Perdew-Burke-Ernzerhof (PBE) functional to account for electron exchange and

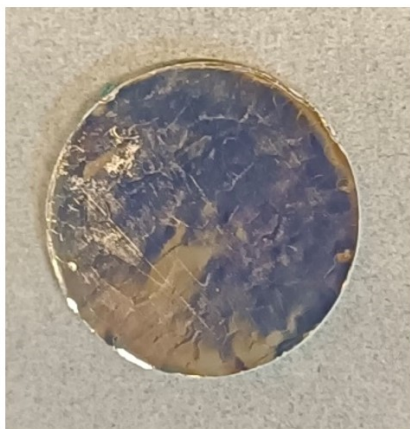
correlation phenomena. A stringent cutoff energy of 500 eV for the plane-wave basis set was established to ensure the accuracy of the calculations. The self-conjugate field (SCF) tolerance is 1×10^{-6} eV. The Brillouin zone is sampled in a $(5 \times 5 \times 5)$ grid. The core electrons are treated with ultra-soft pseudopotentials. The molecular adsorption energy (ΔE_{ad}) of the surface was calculated by the equation (1).

$$\Delta E_{ad} = E_{total} - E_{surf} - E_{Na} \quad (1)$$

Where E_{surf} and E_{total} are the total energies of the surface before and after the adsorption, and E_{Na} is the energy of the adsorbed molecules. The adsorption structure energy is based on the lowest energy state $\Delta E = 0.0000$, where ΔE is the difference between the total energy and the lowest energy state.

Supporting Figures

a



b

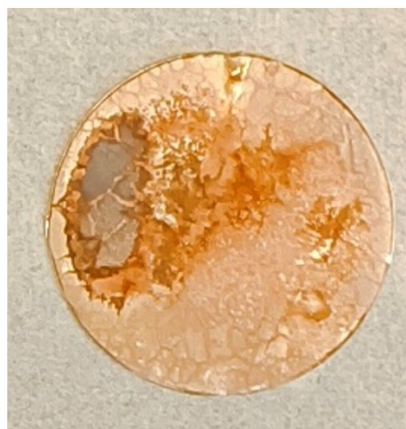


Figure S1. Optical image of (a) bare Na and (b) Na reacting directly with FEMC.



FEMC:DME

Figure S2. Optical image of FEMC:DME at different ratios.

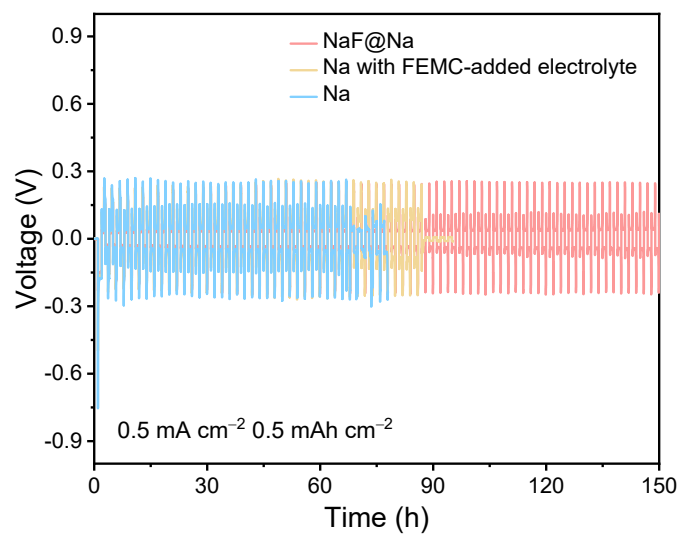


Figure S3. Time-voltage profiles of the investigated system.

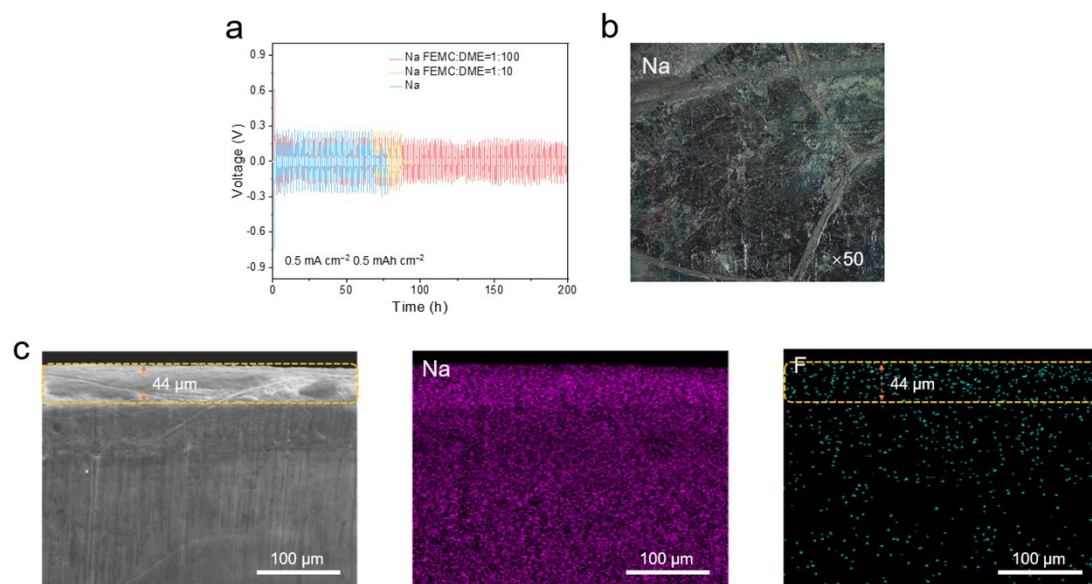


Figure S4. (a) Time-voltage profiles with different solvent ratios. (b) Microscopic images of Na at $50\times$ magnification. (c) Cross-section EDS elemental mapping of NaF@Na.

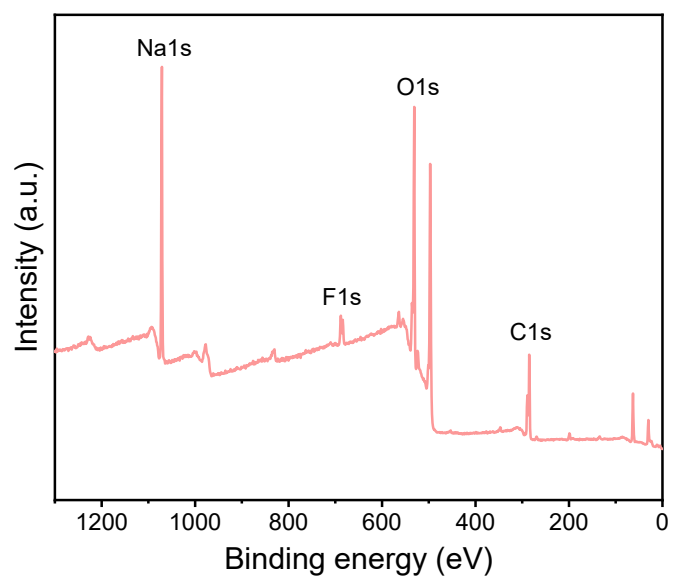


Figure S5. Survey spectrum of NaF@Na.

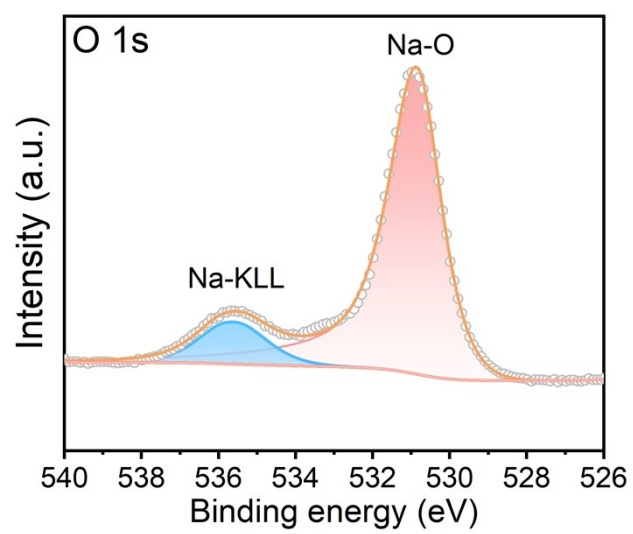


Figure S6. O 1s spectrum of NaF@Na.

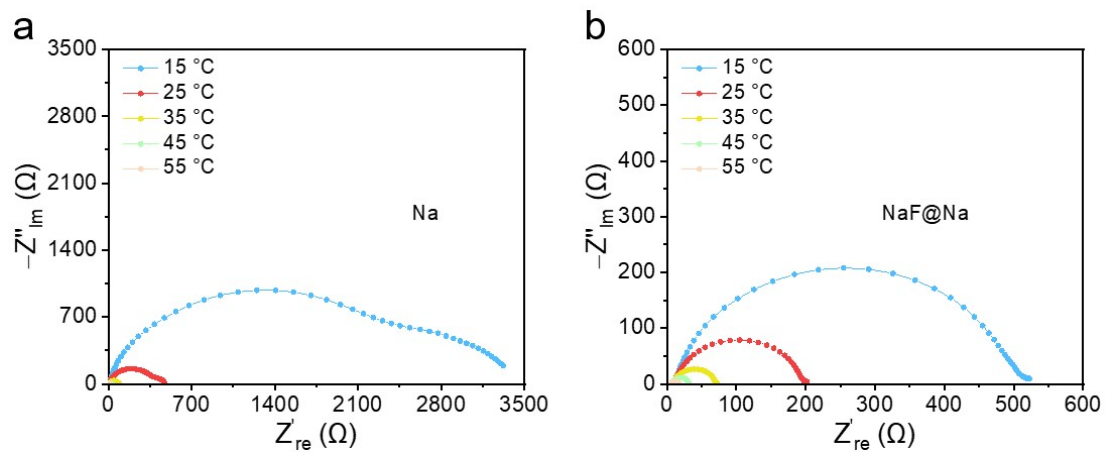


Figure S7. The EIS spectra of (a) pristine Na and (b) NaF@Na electrodes at different temperatures.

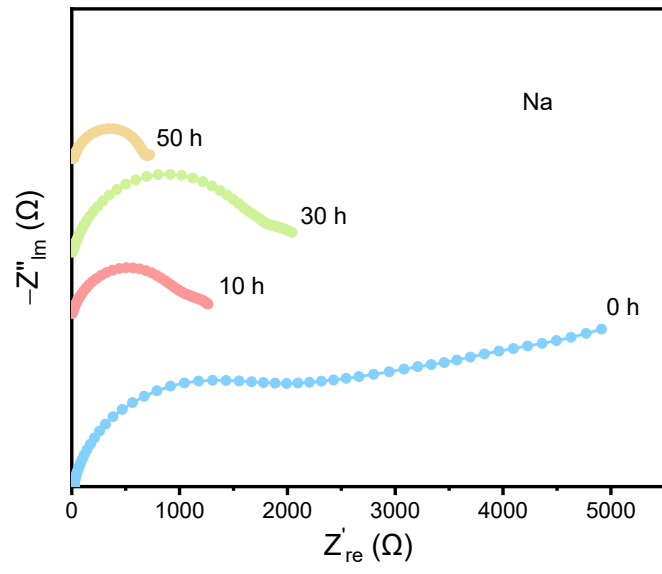


Figure S8. The EIS spectra of pristine Na symmetric cell at different cycles.

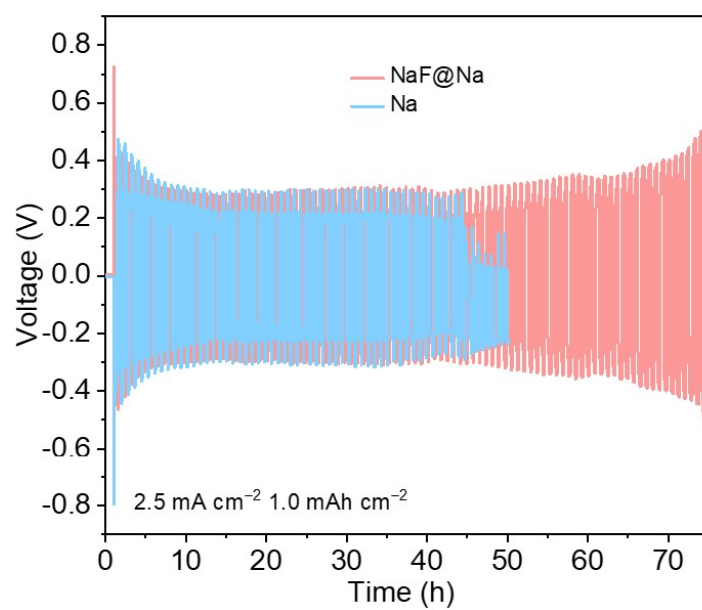


Figure S9. Time-voltage profiles of NaF@Na and Na symmetric cells at 2.5 mA cm^{-2} and 1.0 mAh cm^{-2} .

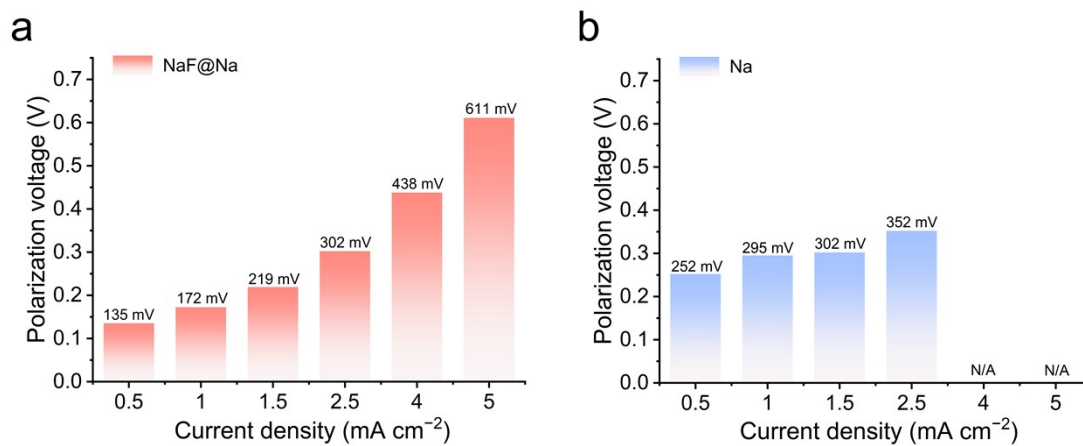


Figure S10. Polarization voltages at various current densities of (a) NaF@Na and (b) Na symmetric cells.

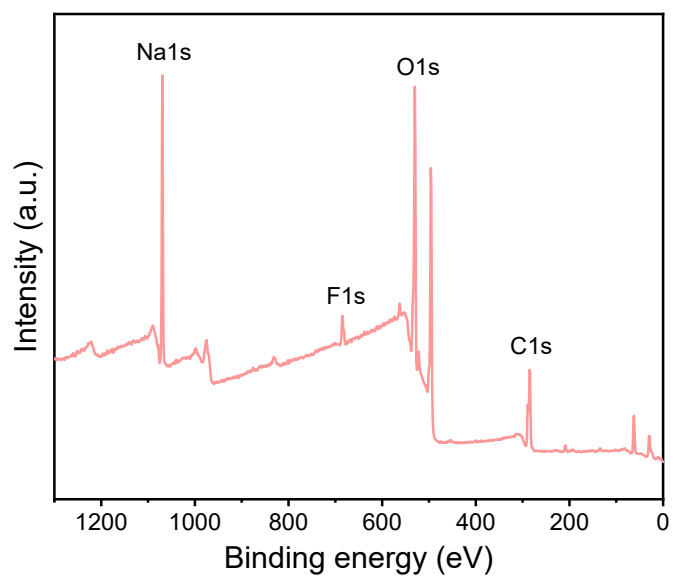
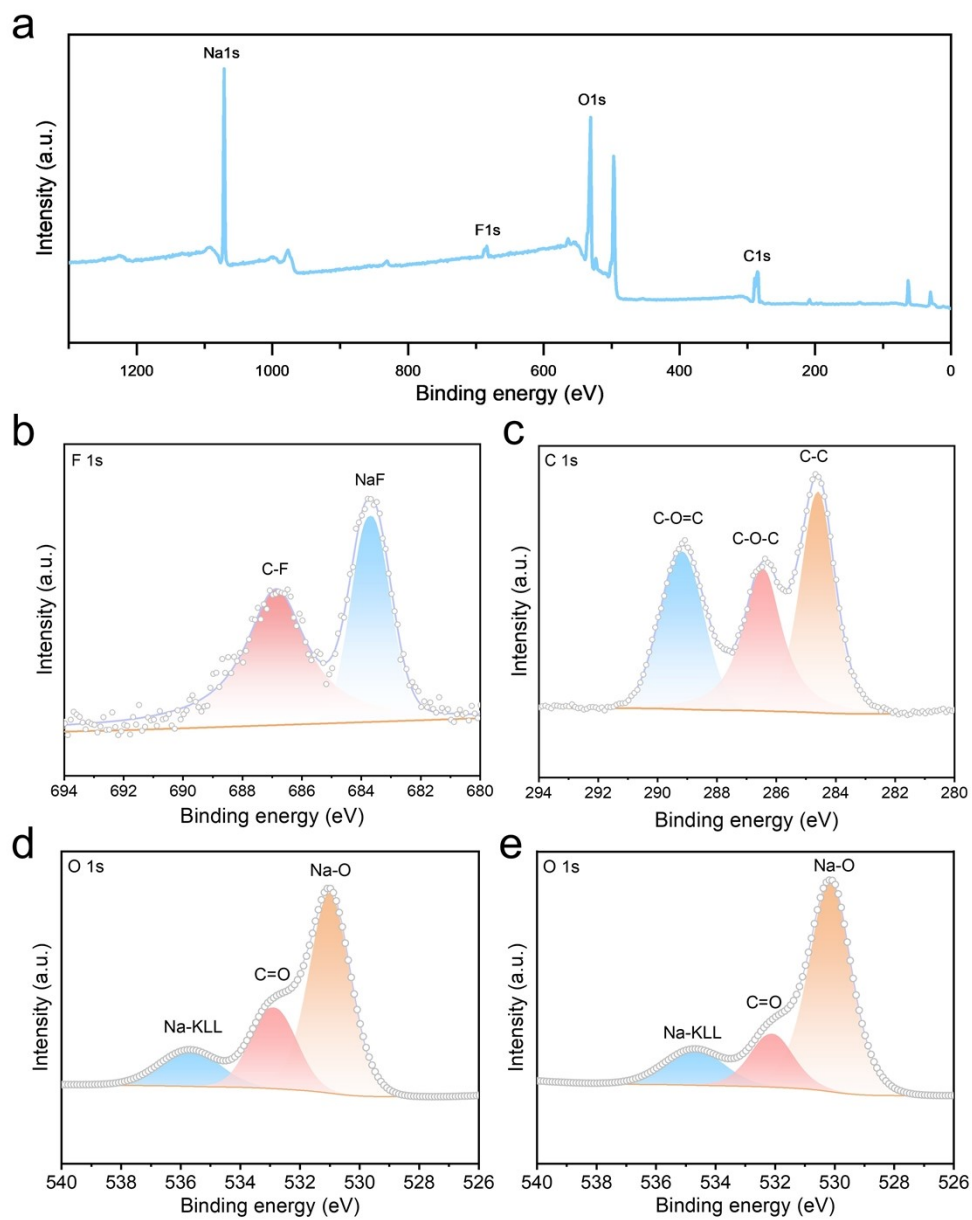


Figure S11. Survey spectrum of cycled NaF@Na.



Fi

Figure S12. (a) Survey, (b) F 1s, (c) C 1s, and (d) O 1s spectra of cycled Na. (e) O 1s spectrum of cycled NaF@Na.

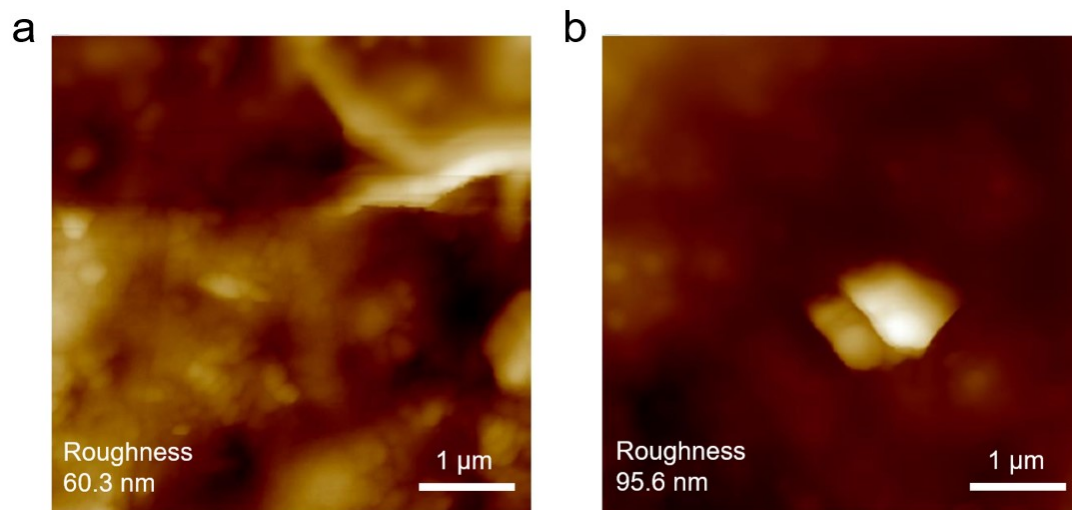


Figure S13. 2D morphology and corresponding roughness of (a) NaF@Na and (b) Na after cycling.



Figure S14. Optical image of NaF@Na immersed in electrolyte.

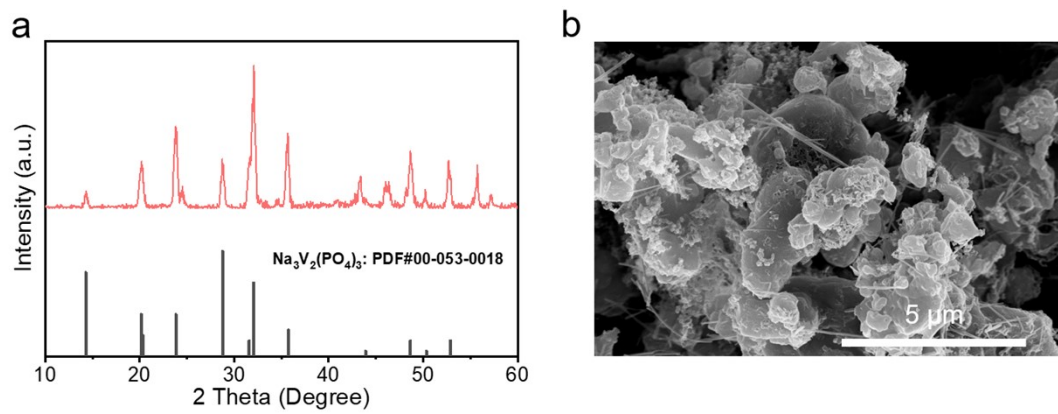


Figure S15. (a) XRD pattern and (b) SEM image of NVP powder.

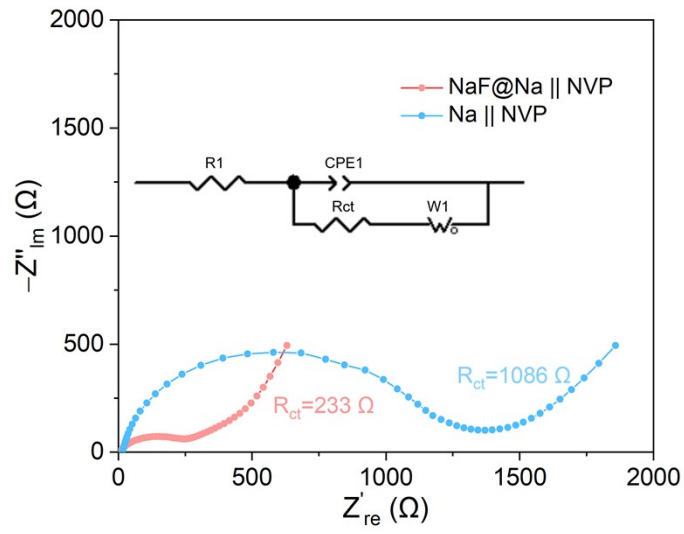


Figure S16. The EIS spectra of NaF@Na || NVP and Na || NVP full cells.